# A 3-D Integral Equation-Based Approach to the Analysis of Real-Life MMICs—Application to Microelectromechanical Systems

Marco Farina, *Member, IEEE,* and Tullio Rozzi, *Fellow, IEEE*

***Abstract*—In this paper, we introduce a three-dimensional method-of-moments approach, suitable for the analysis of real-life monolithic circuits for microwaves/millimeter waves. It shares the flexibility and the efficiency of the currently available spectral-domain commercial simulators, while allowing all metallizations to have finite thickness and finite conductivity and the ability to handle dielectric discontinuities. The method is successfully applied to several structures, like metal–insulator–metal capacitor, spiral inductors, and microelectromechanical capacitive switches in the 1–50-GHz frequency range.**

***Index Terms*—MEMS, method of moments, MMICs, switches.**

## I. Introduction

THE method of moments (MoM) applied to spectral-domain (SD) integral equations is one of the most successful tools in the analysis of printed multilayer circuits. The number of commercially available software packages exploiting this philosophy bears witness to such success.

The most popular electromagnetic tools rely basically on the approach described in [1], adopting the efficiency-enhanced algorithm introduced in [2] and the method detailed in [3], allowing vias to be treated by means of constant vertical currents. The main limitation of these software packages is that, in principle, they are not able to rigorously handle thick lossy conductors, even if such a limitation is partially overcome by some sort of expedient. Surface impedances were used, e.g., in [4] in order to include conductor losses, and metallizations with finite thickness are often modeled by means of boxes constituted by infinitely thin conductors or introducing a number of vias between parallel thin conductors. While this kind of device leads to satisfactory results for microstrip structures, it proves to be sometimes inaccurate in coplanar waveguide (CPW) structures, at least whenever spacing between conductors is comparable to or smaller than the conductor thickness. The reason for this is that the current distribution over the conductor thickness plays a role in describing the effective field distribution over the structure cross section.

In [5], we introduced a different point of view, leading to a two-dimensional (2-D) general approach to the modeling of a lossy planar structure. In [6], this was also extended to include linear active effects and used to model millimeter wave field-effect transistors (FETs). In [7], the first three-dimensional (3-D) formulation was proposed by adopting the excitation scheme introduced in [8], namely the travelling-wave excitation, obtaining satisfactory results. However, it is known that this kind of excitation suffers from some limitations, mainly due to the need for considering waves impinging from infinity, and the resulting formulation lacks, in our opinion, the flexibility needed for integration in a commercial software framework.

In this paper, a 3-D formulation is developed by the more conventional delta-gap excitation scheme [9], which is the one currently used by commercial software packages: by adopting this scheme, a general purpose program including a simple editor that allows one to deal with general topologies has been realized. Using this approach, thick lossy conductors may be analyzed, as well as dielectric discontinuities: the technique has been successfully applied to several structures, such as the metal–insulator–metal (MIM) capacitor, spiral inductors, and CPWs.

As key examples, we report the simulation of a few microelectromechanical (MEM) capacitive switches, as MEM devices are attracting more and more attention, providing a new class of RF devices [10] and some new system design possibilities, which at the moment are only limited by challenging technological and modeling issues. The following examples have been chosen because, in spite of their simplicity—often a simple lumped element equivalent circuit may well do—they are hardly addressed by the available approaches. In fact, while the conventional SD approaches are potentially faced with their limitation in handling lossy metals with finite thickness, techniques relying on some space/time discretization, e.g., finite-differences (FDs) or the transmission-line method (TLM), fail or simply become inefficient due to the aspect ratio of the involved geometrical dimensions. In this context, according to our preliminary results, the proposed approach seems to be an ideal candidate as a computer-aided design (CAD) tool in this forthcoming endeavor.

## II. Theory

According to the strategy adopted in [5] for 2-D structures, as a first step the dyadic Green's function (DGF) of the dielectric multilayer structure has to be calculated. This step is common to standard MoM approaches, such as [1]; however, in the present approach, the DGF has to relate the electric field in the dielectric stack to *volume* currents. As an additional difficulty, this representation has to be valid even in the source region: the issue is investigated in [11].

Manuscript received March 28, 2001; revised August 1, 2001.

The authors are with the Dipartimento di Elettronica ed Automatica, University of Ancona, 60131 Ancona, Italy (e-mail: m.farina@ee.unian.it).

Publisher Item Identifier S 0018-9480(01)10473-4.

Consequently

$$\mathbf{E}(\mathbf{r}) = -\iiint_V d\mathbf{r}'\mathbf{Z}(\mathbf{r}, \mathbf{r}') \cdot \mathbf{J}(\mathbf{r}') \tag{1}$$

where $V$ is the volume where currents are nonvanishing and $\mathbf{Z}$ is the needed DGF. $\mathbf{Z}$ also includes dielectric losses by the usual definition of complex permittivity.

The very nature of volume currents is specified by imposing Ohm's law to be satisfied within the lossy conductors: this condition replaces the vanishing of the tangential electric fields, as used by standard SD MoM.

Actually, there is no need to restrict our attention to conduction currents: more generally, $\mathbf{J}$ could be also a displacement current used to model a finite dielectric body. For the general case of a lossy dielectric region, we impose the relationship

$$\mathbf{E}(\mathbf{r}) = \frac{\mathbf{J}(\mathbf{r})}{j\omega\varepsilon_0(\tilde{\varepsilon}(\mathbf{r}) - \tilde{\varepsilon}'(\mathbf{r}))} \tag{2}$$

where $\tilde{\varepsilon}$ is the complex permittivity of the additional dielectric, while $\tilde{\varepsilon}'$ is that of the embedding medium. The difference between the two complex permittivities is needed as currents due to $\tilde{\varepsilon}'$ are already embodied in the definition of $\mathbf{Z}$. A similar condition was used in [14] to model dielectric bricks. Actually, as (2) implies Ohm's law, it is also used to model thick lossy conductors, while for ideal conductors it is replaced by the condition $\mathbf{E} = 0$ over the whole metal volume.

In order to obtain a deterministic integral equation, some kind of known excitation has to be imposed: in this paper we use the conventional delta-gap excitation scheme introduced in [9]. The whole structure is assumed to be enclosed between electric walls (however, top and bottom covers may also be infinite dielectric layers) and, at some point along the feeding lines, a constant electric field, orthogonal to a virtual plane cutting the line conductor, is applied. Such a plane may be defined at an arbitrary position and along any of the three directions.

Hence the excitation field is

$$\mathbf{E}_0(\mathbf{r}) = -\delta(v - v_0)\mathbf{u}, \qquad \text{if } \mathbf{r} \in \text{feeding line } p \tag{3}$$

where $v = x$, $y$, or $z$ and $\mathbf{u}$ is the direction normal to the defined plane (see Fig. 1). This is a unitary voltage generator applied at an arbitrary reference plane defining an accessible port $p$; usually, even if not necessarily, the plane coincides with one of the enclosing walls (edge and via ports), so to have ground referenced quantities in the subsequent network calculations.

Summarizing, the condition (2) and the excitation (3) are applied to (1), providing the integral equation

$$\iiint_V d\mathbf{r}' \left[\mathbf{Z}(\mathbf{r}, \mathbf{r}') + \frac{1}{j\omega\varepsilon_0(\tilde{\varepsilon}(\mathbf{r}) - \tilde{\varepsilon}'(\mathbf{r}))}\mathbf{I}(\mathbf{r}, \mathbf{r}')\right] \cdot \mathbf{J}(\mathbf{r}') = \delta(v - v_0)\mathrm{rect}(p)\mathbf{u} \tag{4}$$

where $\mathbf{I}$ is the identity operator and $\mathrm{rect}(p)$ is a function of unit amplitude not vanishing only along the cross section of the feeding line at port $p$. Equation (4) must be solved within the volume of the conductors and of the finite dielectric regions—namely, dielectrics not extending up to the enclosure walls.

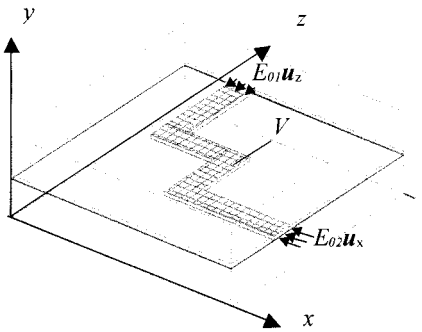


Fig. 1. 3-D structure involving finite thickness conductors, with delta-gap excitation.

To this aim, the MoM is applied to (4), expanding the unknown currents as

$$\begin{aligned} J_x(x, y, z) &= \sum_{i=1}^{N_x-1}\sum_{j=1}^{N_y}\sum_{k=1}^{N_z} \mathrm{PWS}(x, x_i, x_{i+1}) \\ &\quad \cdot rect(y - y_j)\mathrm{rect}(z - z_k) \\ J_y(x, y, z) &= \sum_{i=1}^{N_x}\sum_{j=1}^{N_y}\sum_{k=1}^{N_z} \mathrm{rect}(x - x_i) \\ &\quad \cdot \mathrm{rect}(y - y_j)\mathrm{rect}(z - z_k) \\ J_z(x, y, z) &= \sum_{i=1}^{N_x}\sum_{j=1}^{N_y}\sum_{k=1}^{N_z-1} \mathrm{rect}(x - x_i) \\ &\quad \cdot \mathrm{rect}(y - y_j)PWS(z, z_k, z_{k+1}) \end{aligned} \tag{5}$$

where $\mathrm{PWS}(u, u_i, u_{i+1})$ are asymmetrical piecewise sinusoidal functions with argument $k_o$, the vacuum wavenumber, and $N_x$, $N_y$, and $N_z$ are the number of subsection intervals. According to (5), every current component is assumed to have a piecewise constant dependence on the y coordinate. Note that substitution of (5) into (4) involves a set of integrals that can be analytically solved.

The solution of (4) yields the complete current distribution over the thick lossy metals and dielectric bodies, as well as, by means of (1), the electric-field distribution everywhere in the dielectric stack. By integrating the current distributions along the sections where the ports are defined, one obtains the network admittance ($Y$) parameters as

$$y_{ij} = I_i\Big|_{v_k = \begin{cases} 1 & \text{if } k=j \\ 0 & \text{otherwise} \end{cases}}, \qquad k, i, j = 1, \ldots, N \tag{6}$$

where $N$ is the number of ports, $I_i$ is the current at the $i$th port, and $v_k$ is the voltage generator at the $k$th port.

Defining the ports leads to a local discontinuity: this is due to several effects, like the excitation of high-order modes and the presence of lateral walls. Such a discontinuity may sometimes model an actual discontinuity encountered in the circuit being modeled; if this is not the case, the discontinuity has to be evaluated and removed by means of one of the standard deembedding algorithm. A new algorithm showing some attractive features with respect to the existing ones is discussed in [12] and is used in the present work.

Using expansion (5) leads to complete freedom in the class of devices that the method can successfully address. Modeling of skin effect is rigorously accounted for, the only requirement

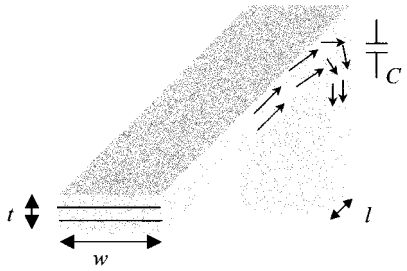


Fig. 2. Vertical sharp discontinuity.

being that the number of $y$ subsections be enough to roughly approximate the actual current distribution—namely, that each subsection be smaller than the skin depth. If this is not the case, losses usually appear to be underestimated.

A fine $y$ subsectioning is also needed whenever sharp vertical discontinuities are encountered, like in vias or contacts between conductors lying on different layers (see, e.g., Fig. 2). A coarse $y$ subsectioning results in a large parasitic (unphysical) series capacitance expressing the inability to correctly model the vertical gradient of the current density: while this capacitance does not affect high-frequency results, it may heavily influence low-frequency results. Such a capacitance has been empirically determined to be roughly given by

$$\mathrm{C} \approx \varepsilon_{\mathrm{r}} \varepsilon_0 l w N_y k / t \tag{7}$$

where $k$ is an empirical factor (of order of magnitude about ten), $N_y$ is the number of vertical subsections of the upper conductor, and $l$, $w$, and $t$ are shown in Fig. 2. Hence, it is apparent that C could be made arbitrarily large by increasing $N_y$. There is no counterpart of this undesired phenomenon in the so-called 2.5-D approaches, the thickness $t$ being zero.

Actually increasing Ny, i.e., the number of vertical "slices," may result in a large computational effort.

An alternative approach is to use a sort of "deembed" algorithm, whenever possible: a separate structure is specifically designed to evaluate the parasitic capacitance by means of a low-frequency simulation. Such a capacitance is hence subtracted at circuit level by cascading a negative capacitance to the resulting network. The feasibility of this alternative route is determined by whether the point of appearance of the capacitance is externally accessible or not.

An expedient $y$-discretization would theoretically reduce or eliminate this effect; actually, the functional form of the Green's function of a stratified medium limits the class of the expanding functions that can be analytically integrated.

## III. Results

By using the theory described in the previous section, a general purpose program, i.e., EM3DS, has been developed and used successfully to study several passive structures.

Fig. 3 shows the seven-turn spiral inductor reported in [15]: the inductor is fabricated on 10-Ω-cm silicon substrate ($\varepsilon_{\mathrm{r}} = 11.9$, 500- $\mu$m thick), over a 4.5-$\mu$m oxide layer ($\varepsilon_{\mathrm{r}} = 3.9$), using aluminum electrodes ($\sigma = 3\ 10^7$ S/m) 1-$\mu$m thick. Other topological parameters are 13-$\mu$m width, 7-$\mu$m spacing, and 300-$\mu$m outer dimension. Fig. 4 shows a comparison between measured and modeled quality factor $Q$ defined according to

$$Q = \mathrm{Im}(Y11)/\mathrm{Re}(Y11). \tag{8}$$

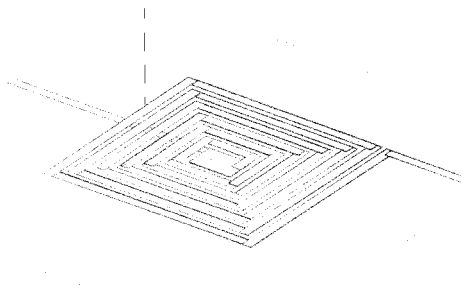

Fig. 3. Seven-turn silicon spiral inductor: 3-D view.

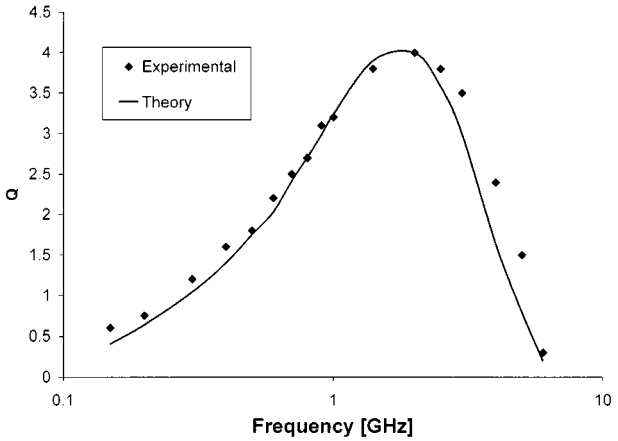


Fig. 4. Comparison between measured and computed values for the quality factor $Q$ of the inductor shown in Fig. 3.

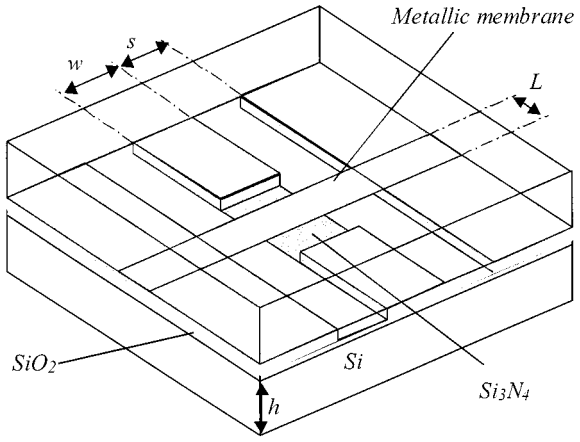


Fig. 5. Geometry of the MEM [13] ("on" position): $w = 100$ $\mu$m, $s = 60$ $\mu$m, $L = 80$ $\mu$m, $h = 400$ $\mu$m; the Au metallization is 2.3-$\mu$m thick, while the metallic membrane is 2-$\mu$m thick; the switch electrode is 0.8-$\mu$m thick, covered by a 0.15-$\mu$m thin film of $\mathrm{Si_xN_y}$ ($\varepsilon_{\mathrm{r}} = 7.6$). The nominal gap is 1.5 $\mu$m. The switch is on the top of a 0.4-$\mu$m silicon dioxide insulating layer ($\varepsilon_{\mathrm{r}} = 3.9$). For the buffer $\varepsilon_{\mathrm{r}} = 11.9$, $\sigma = 0.033$ S/m. The whole structure is 160-$\mu$m long.

The agreement is quite good. In this example, the parasitic capacitance due to the sharp vertical discontinuity—the underpass involving the via—was important due to the small area of the via. Results plotted in Fig. 4 were obtained after evaluating and removing such a capacitance ($\mathrm{C} = 2.024$ pF) according to the procedure described in the previous paragraph.

As to the modeling of dielectric discontinuities, several tests have been performed, including a MIM capacitor $30 \times 30$ $\mu\mathrm{m}^2$,

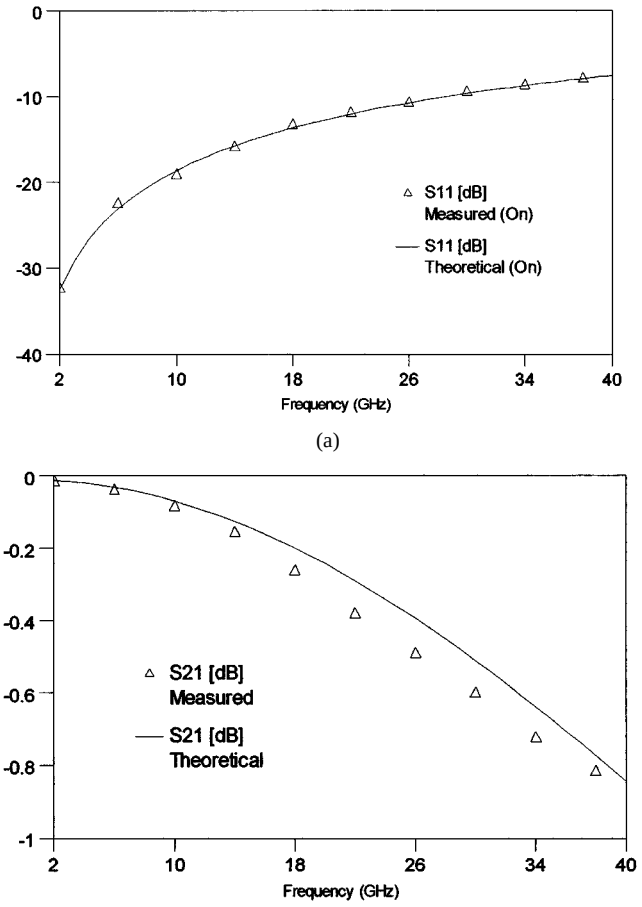


Fig. 6. Return loss and insertion loss for the "on" state: comparison between (a) theoretical and (b) experimental data [13].

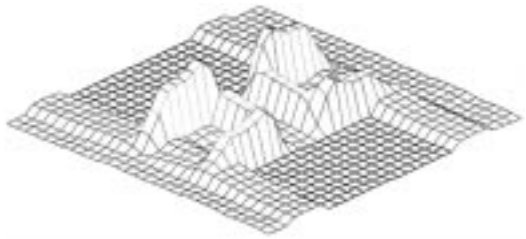

Fig. 7. Total current density distribution over the bridge in the "on" state at 40 GHz.

involving a 0.1-$\mu$m-thick GaAs dielectric brick: the parallel plate formula predicts a capacitance $C = 1.028$ pF, while results from low-frequency electromagnetic simulation gave $C = 1.027$ pF.

A more interesting test-bed is the analysis of MEM devices, as the thickness and the conductivity of the metallizations may hardly be neglected. A typical MEM capacitive switch [13] is depicted in Fig. 5: it is shown in its unactuated ("on") position. In such a case, the structure is similar to a bridge on a thick, lossy CPW. As the bridge capacitance is relatively small, removing the port discontinuity by means of a correct deembedding procedure is generally very important. The metal thickness may play a major role in this case, potentially causing inaccuracy in standard 2.5-D MoM approaches. Fig. 6 reports a comparison between the experimental results of [13] and the theoretical ones obtained by the proposed method.

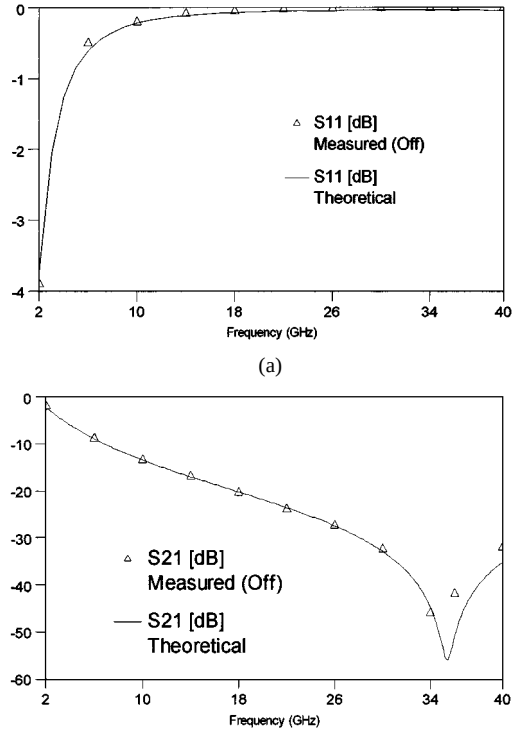


Fig. 8. Return loss and insertion loss for the "off" state: comparison between: (a) theoretical and (b) experimental data [13].

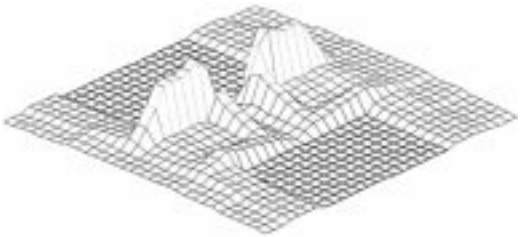

Fig. 9. Total current density distribution over the bridge in "off" state at 40 GHz.

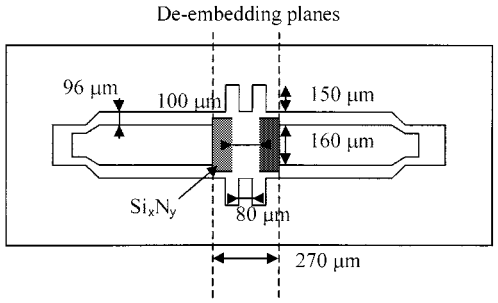


Fig. 10. Inductively tuned high-isolation $X$-band switch [16]: a 150 -$\mu$m-long high-impedance line is added between the bridge and the ground to enhance the bridge inductance.

Fig. 7 shows the distribution of the total current density over the bridge in the "on" state at 40 GHz. While in the lower frequency range the distribution is completely symmetrical, only a slight asymmetry appears at 40 GHz, suggesting just a limited interaction between the impinging mode of the coplanar structure (left-hand side) and the upper bridge.

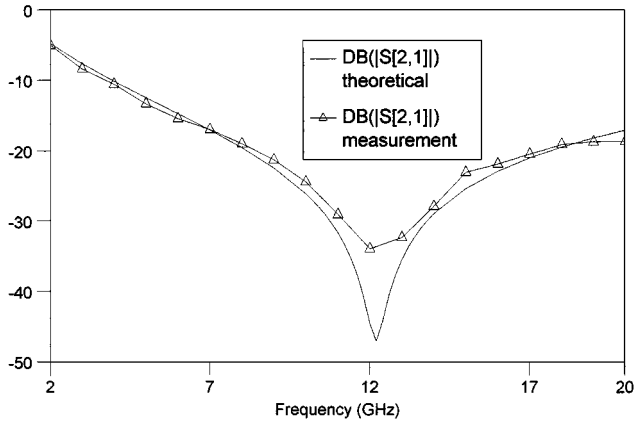


Fig. 11. Comparison between theoretical and experimental [16] data for the structure shown in Fig. 8 ("off" state).

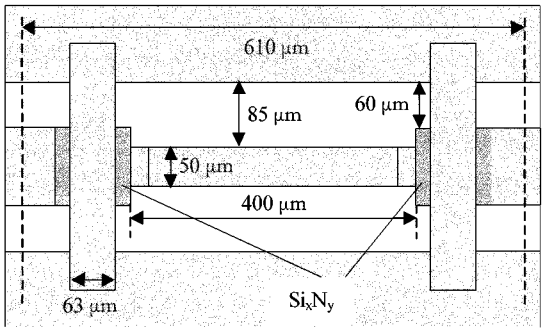


Fig. 12. Double switch [16]: two switches are connected by a 400-$\mu$m-long high-impedance line in order to reduce return loss in "on" state while obtaining high insulation in the "off" state.

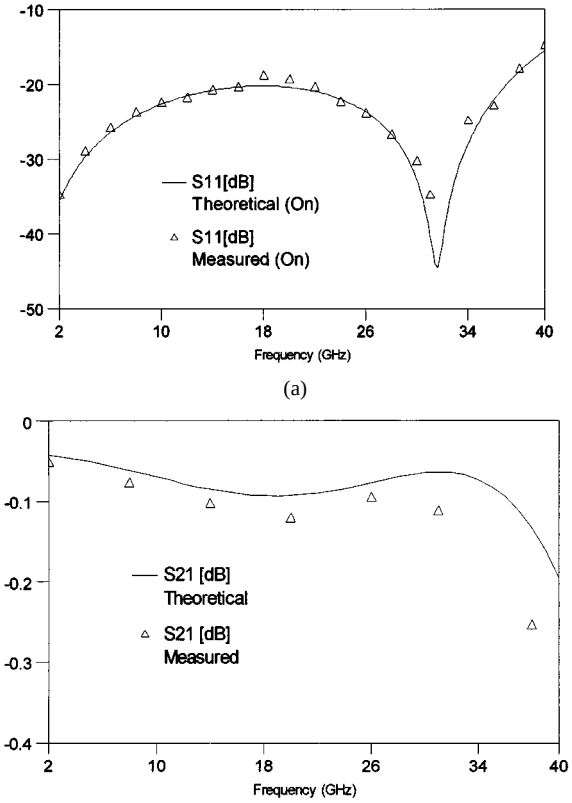


Fig. 13. Return loss and insertion loss for the "on" state: comparison between: (a) theoretical and (b) experimental data [16].

The actuated ("off") position is the one that usually poses a major challenge to the FD and TLM methods: in this state, an electrostatic potential snaps down the metallic membrane, now acting as a large shunt capacitance.

A thin film (0.1 $\mu$m) of silicon nitride that prevents the upper membrane from sticking to the lower electrode now plays a major role: discretizing the whole structure as required by standard FD and TLM methods may lead to inefficient or unstable solutions, due to the critical aspect ratio.

Moreover, the shunt capacitance, assuming large values (it may range in the order of some picofarads), is responsible for long transient oscillations in time-domain methods.

Fig. 8 shows a comparison between experimental data [13] and our theoretical data for the return and insertion loss for the switch in the "off" state. In both cases (on and off), theoretical results show excellent agreement with the experimental ones, while being obtained without any "trimming-to-fit" procedure. Fig. 9 shows the current distribution over the bridge in the "off" position: as expected, a strong asymmetry appears, the current being concentrated to the left hand side, since this edge acts as a short for the incoming wave.

Fig. 10 shows a slightly more complicated structure, namely an inductively tuned high isolation capacitive switch for $X$-band application [16]. In this kind of device, higher isolation is obtained by increasing the series inductance of the switch so as to lower the resonant frequency. The needed large series inductance is obtained by inserting a short high-impedance transmission line between the bridge and the MEM ground.

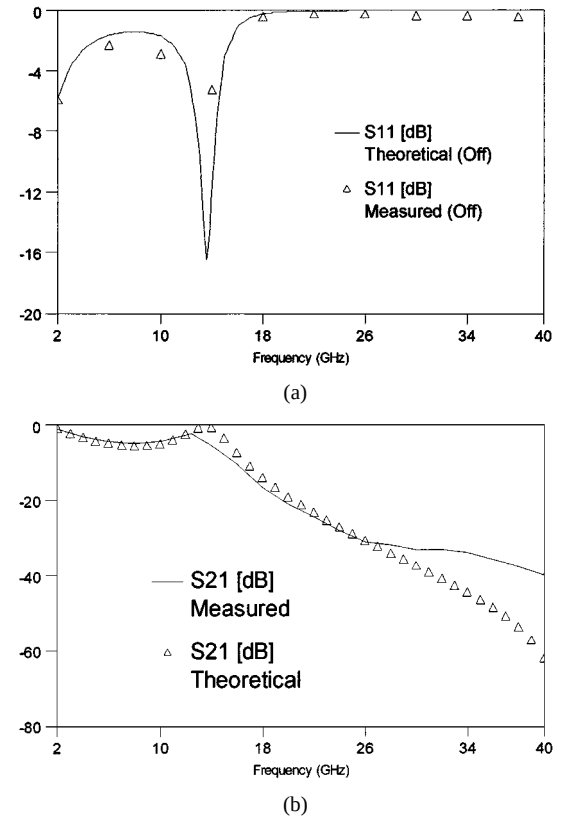


Fig. 14. Return loss and insertion loss for the "off" state: comparison between: (a) theoretical and (b) experimental data [16].

The comparison between the experimental data by [16] and the theoretical data in Fig. 11 also shows in this case satisfactory agreement.

The time needed for the analysis of the above structures ranges around 1 h for 40 frequency points on a Pentium III 600-MHz processor.

As a last example, Fig. 12 shows a double switch described in [16] obtained by cascading two switches and a high impedance line, so to achieve low return loss in the "on" state and high insulation in the "off" state. Comparison with experimental results are reported for the "on" and the "off" states in Figs. 13 and 14, respectively.

## IV. Conclusion

A general 3-D integral equation approach for the modeling of passive MMIC circuits involving thick lossy conductors and dielectric discontinuities has been introduced. Sharing several steps with the MoM currently used by available commercial software packages, the algorithm is flexible and able to handle complex structures.

In order to validate the method, several structures were analyzed. In this paper, we reported the simulation of MEM switches in their "on" and "off" states: the excellent results validate this approach as an efficient tool for the CAD of MEM structures.

## Acknowledgment

The authors would like to thank L. Zampetti for providing valuable data and discussions on some of the examples reported in this paper.

## References

[1] J. C. Rautio and R. F. Harrington, "An electromagnetic time–harmonic analysis of shielded microstrip circuits," *IEEE Trans. Microwave Theory Tech.*, vol. MTT-35, pp. 726–730, Aug. 1987.

[2] A. Hill and V. K. Tripathi, "An efficient algorithm for the three-dimensional analysis of passive microstrip components and discontinuities for microwave and millimeter-wave integrated circuits," *IEEE Trans. Microwave Theory Tech.*, vol. 39, pp. 83–91, Jan. 1991.

[3] T. Becks and I. Wolff, "Analysis of 3-D metallization structures by a full-wave spectral domain technique," *IEEE Trans. Microwave Theory Tech.*, vol. 40, pp. 2219–2327, Dec. 1992.

[4] J. C. Liou and K. M. Love, "Analysis of slow wave transmission lines on multi-layered semiconductor structures including conductor loss," *IEEE Trans. Microwave Theory Tech.*, vol. 41, pp. 824–829, May 1990.

[5] M. Farina, G. Gerini, and T. Rozzi, "Efficient full-wave analysis of stratified planar structures and unbiased TW-FET," *IEEE Trans. Microwave Theory Tech.*, vol. 43, pp. 1322–1329, June 1995.

[6] M. Farina and T. Rozzi, "Electromagnetic modeling of linear pHEMT's for millimeter waves," in *IEEE MTT-S Int. Microwave Symp. Dig.*, vol. 3, Boston, MA, June 2000, pp. 1801–1804.

[7] ——, "A full-wave approach to the modeling of discontinuities of real conductors in planar lossy lines for MMIC applications," in *IEEE MTT-S Int. Microwave Symp. Dig.*, Baltimore, MD, June 7–12, 1998, pp. 1555–1558.

[8] R. W. Jackson and D. M. Pozar, "Full-wave analysis of microstrip open-end and gap discontinuities," *IEEE Trans. Microwave Theory Tech.*, vol. MTT-33, pp. 1036–1042, Oct. 1985.

[9] L. P. B. Katehi and N. G. Alexopoulos, "Frequency-dependent characteristics of microstrip discontinuities in millimeter-wave integrated circuits," *IEEE Trans. Microwave Theory Tech.*, vol. MTT-33, pp. 1029–1035, Oct. 1985.

[10] E. R. Brown, "RF–MEMS switches for reconfigurable integrated circuits," *IEEE Trans. Microwave Theory Tech.*, vol. 46, pp. 1868–1880, Nov. 1998.

[11] T. Rozzi and M. Farina, *Advanced Electromagnetic Analysis of Passive and Active Planar Structures*. London, U.K.: IEE Press, 1999.

[12] M. Farina and T. Rozzi, "A short-open deembedding technique for method of moments based electromagnetic analyzes," *IEEE Trans. Microwave Theory Tech.*, vol. 49, pp. 624–628, Apr. 2001.

[13] J. B. Muldavin and G. M. Rebeiz, "High-isolation CPW MEMS shunt switches—Part 1: Modeling," *IEEE Trans. Microwave Theory Tech.*, vol. 48, pp. 1045–1052, June 2000.

[14] T. Vaupel and V. Hansen, "Electrodynamic analysis of combined microstrip and coplanar/slotline structures with 3-D components based in a surface/volume integral-equation approach," *IEEE Trans. Microwave Theory Tech.*, vol. 47, pp. 1788–1800, Sept. 1999.

[15] C. P. Yue and S. S. Wong, "Physical modeling of spiral inductors on silicon," *IEEE Trans. Electron Devices*, vol. 47, pp. 560–568, Mar. 2000.

[16] J. B. Muldavin and G. M. Rebeiz, "High-isolation CPW MEMS shunt switches—Part II: Design," *IEEE Trans. Microwave Theory Tech.*, vol. 48, pp. 1053–1056, June 2000.

**Marco Farina** (M'98) received the M.Eng. degree in electronics (*summa cum laude)* and the Ph.D. degree from the University of Ancona, Ancona, Italy, in 1990 and 1995, respectively.

From 1991 to 1992, he was a Technical Officer in the Italian Army. Since 1992, he has been with the Department of Electronics and Automatics, University of Ancona, where he is currently an Assistant Professor. He is also a consulting Engineer in electronics. He co-authored *Advanced Electromagnetic Analysis of Passive and Active Planar Structures* (London, U.K.: IEE Press, 1999).

**Tullio Rozzi** (M'66–SM'74–F'90) received the Dottore degree in physics from the University of Pisa, Pisa, Italy, in 1965, the Ph.D. degree in electronic engineering from The University of Leeds, Leeds, U.K., in 1968, and the D.Sc. degree from the University of Bath, Bath, U.K., in 1987

From 1968 to 1978, he was a Research Scientist at the Philips Research Laboratories, Eindhoven, The Netherlands. In 1975, he spent one year at the Antenna Laboratory, University of Illinois at Urbana-Champaign. In 1978, he obtained the Chair of Electrical Engineering at the University of Liverpool, and, in 1981, the Chair of Electronics and Head of the Electronics Group at the University of Bath, where he was also the Head of the School of Electrical Engineering on an alternate three-year basis. Since 1988, he has been a Professor in the Department of Electronics and Automatics, University of Ancona, Ancona, Italy, where he is also the Head of this department.

Dr. Rozzi was the recipient of the 1975 Microwave Prize presented by the IEEE Microwave Theory and Techniques Society (IEEE MTT-S).